New Phytologist

Research

Leaf venation network architecture coordinates functional trade-offs across vein spatial scales: evidence for multiple alternative designs

Ilaine Silveira Matos[1,2], Mickey Boakye[1], Izzi Niewiadomski[1], Monica Antonio[1], Sonoma Carlos[1], Breanna Carrillo Johnson[1], Ashley Chu[1], Andrea Echevarria[1], Adrian Fontao[1], Lisa Garcia[3], Diana Kalantar[1], Srinivasan Madhavan[1], Joseph Mann[1], Samantha McDonough[1], James Rohde[1], Meg Scudder[1], Satvik Sharma[1], Jason To[1], Connor Tomaka[1], Bradley Vu[1], Nicole Yokota[1], Holly Forbes[4], Mark Fricker[5] and Benjamin Wong Blonder[1]

[1]Department of Environmental Science Policy and Management, University of California Berkeley, Berkeley, CA 94720, USA; [2]School of Biological Sciences, The University of Adelaide, Adelaide, SA, 5005, Australia; [3]Department of Biology, University of New Mexico, Albuquerque, NM 87131, USA; [4]University of California Botanical Garden, Berkeley, CA 94720, USA; [5]Department of Biology, University of Oxford, Oxford, OX1 3RB, UK

Author for correspondence:
Ilaine Silveira Matos
Email: ilaine.matos@gmail.com

Received: *15 February 2024*
Accepted: *16 July 2024*

New Phytologist (2024) **244:** 407–425
doi: 10.1111/nph.20037

Key words: construction cost, damage resilience, damage resistance, functional trade-offs, leaf trait, network architecture, plant hydraulics, venation.

Summary

- Variation in leaf venation network architecture may reflect trade-offs among multiple functions including efficiency, resilience, support, cost, and resistance to drought and herbivory. However, our knowledge about architecture-function trade-offs is mostly based on studies examining a small number of functional axes, so we still lack a more integrative picture of multidimensional trade-offs.
- Here, we measured architecture and functional traits on 122 ferns and angiosperms species to describe how trade-offs vary across phylogenetic groups and vein spatial scales (small, medium, and large vein width) and determine whether architecture traits at each scale have independent or integrated effects on each function.
- We found that generalized architecture-function trade-offs are weak. Architecture strongly predicts leaf support and damage resistance axes but weakly predicts efficiency and resilience axes. Architecture traits at different spatial scales contribute to different functional axes, allowing plants to independently modulate different functions by varying network properties at each scale.
- This independence of vein architecture traits within and across spatial scales may enable evolution of multiple alternative leaf network designs with similar functioning.

Introduction

Substantial variation in leaf venation network architecture exists across plant phylogeny (Fig. 1). Some species have a single vein, while others exhibit complex networks with vein density exceeding 25 mm mm^{-2} (Boyce *et al.*, 2009; Brodribb *et al.*, 2010). Some networks are strictly branching, while others comprise thousands of loops with variable shapes. Variation in network architecture also occurs across vein spatial scales (vein orders or sizes) within a single leaf. For example, in many angiosperms, minor veins form loops, whereas major veins only branch (Blonder *et al.*, 2020). While it is still unclear what evolutionary processes have created such a variety of venation networks (Fujita & Mochizuki, 2006), one leading hypothesis is that different networks may reflect selection to optimize different functions (Roth-Nebelsick *et al.*, 2001; Sack & Scoffoni, 2013; Blonder *et al.*, 2020).

Venation networks may contribute to at least six functional axes (hypotheses expanded in Tables 1, 2): (1) damage resistance to drought (leaf ability to avoid water flow interruption due to xylem conduit implosion or embolism), (2) damage resistance to herbivory (leaf ability to avoid water flow disruption caused by herbivores cutting veins), (3) damage resilience to drought and herbivory (leaf capacity to maintain flow after damages have occurred), (4) flow efficiency (how efficiently water flows through the leaf), and (5) mechanical support (leaf capacity to remain upright in space), which must be traded-off against (6) the leaf construction cost. Due to biophysical and physiological constraints, it might be impossible to construct a network that simultaneously optimizes all functions (Blonder *et al.*, 2018, 2020). For instance, it might be difficult to simultaneously achieve high efficiency (via branching networks) and high resilience (via looping networks), as those functions depend on opposing architectural features (Roth-Nebelsick *et al.*, 2001; Ronellenfitsch &

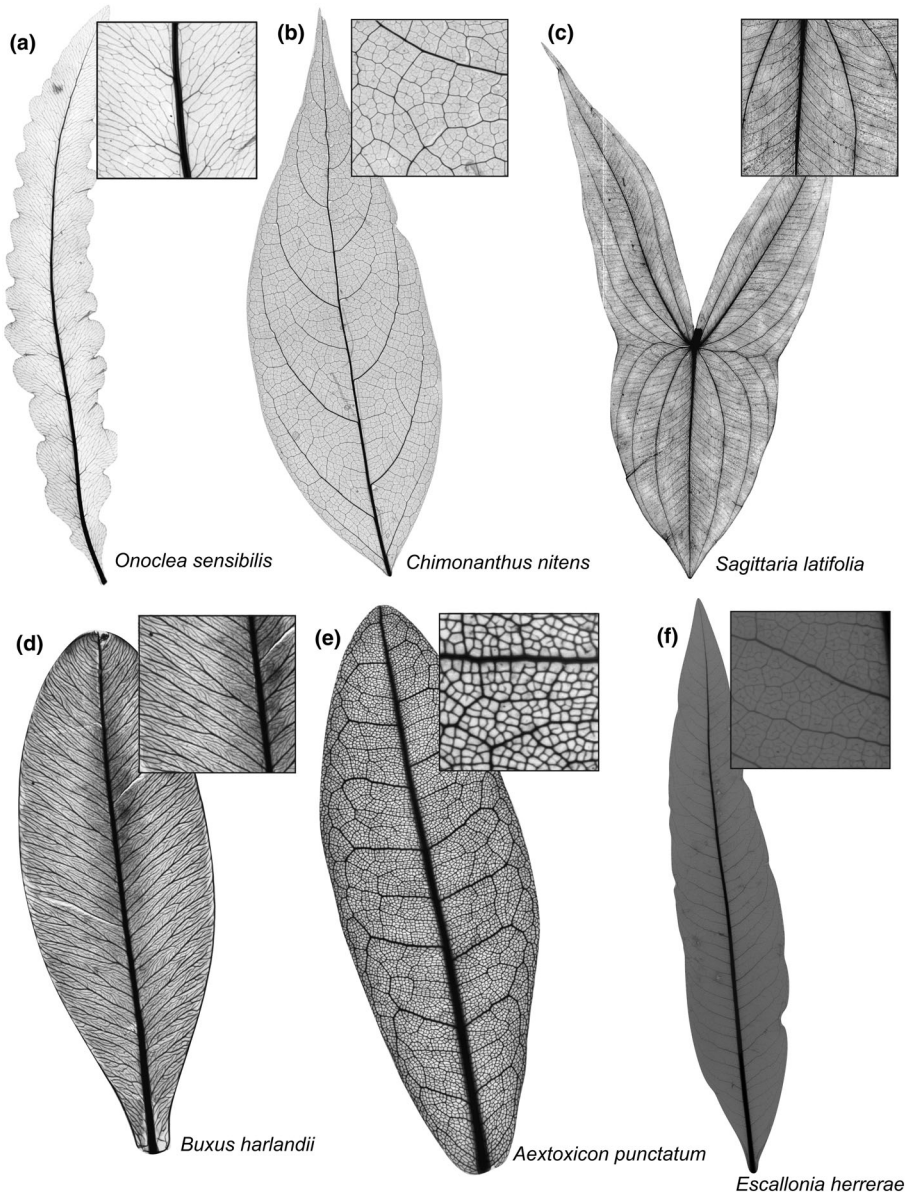

Fig. 1 Examples of variation in leaf venation network architecture across plant clades: (a) Fern: *Onoclea sensibilis* L. (Onocleaceae); (b) Basal angiosperm: *Chimonanthus nitens* Oliv. (Calycanthaceae); (c) Monocot: *Sagittaria latifolia* Willd. (Alismataceae); (d) Basal eudicot: *Buxus harlandii* Hance (Buxaceae); (e) Rosid: *Aextoxicon punctatum* Ruiz & Pav. (Aextoxicaceae); and (f) Asterid: *Escallonia herrerae* Mattf. (Escalloniaceae).

Katifori, 2019). Depending on the selective forces under which plants have evolved, they may have developed different network architectures as compromises among multiple functions.

While it is known that venation architecture traits (Table 3) vary across spatial scales (Blonder *et al.*, 2020), how features at each scale influence different functions remains only partially understood. Some studies propose a functional independence (aka 'labor sharing' Kawai & Okada, 2016, 2018) across spatial scales, where features at different vein orders contribute to different functions (Roth-Nebelsick *et al.*, 2001; Ueno *et al.*, 2006; Sack & Scoffoni, 2013). That is, architecture traits at different vein sizes are uncorrelated, allowing plants to independently regulate different functions at each scale. For example, minor vein density may regulate flow efficiency, while major vein density may influence mechanical properties (Sack & Scoffoni, 2013; Kawai & Okada, 2016). By contrast, there could be an integration across vein orders, where venation traits at different spatial scales are coselected and coordinated to support overall leaf functioning, for example via consistent vein tapering ratios (Price *et al.*, 2007; Savage *et al.*, 2010; Ronellenfitsch *et al.*, 2015). Those scenarios are not mutually exclusive, and it is possible that the degree of integration vs independence among architecture traits vary across species. Most studies examining those trade-offs were limited to a few species, so we still do not know how the architecture-function space is partitioned among phylogenetically distinct taxa with a wide range of network architectures.

Features not related to the venation architecture can also influence leaf functions and may covary, cancel out, or reinforce the architecture-function trade-offs (Table 2). For instance, outside-xylem conductance can be equally or even more important than the vein-mediated transport to determine flow efficiency (Scoffoni *et al.*, 2023). Similarly, chemical defenses may contribute more to herbivory resistance (Agrawal & Fishbein, 2006), than the mechanical defenses provided by the lignified network

Table 1 List of abbreviations and their meaning.

Abbreviation	Meaning
$\Delta K_{leaf_{lamina}}$	Change in leaf hydraulic conductance 48 h after the leaf lamina has been severed
$\Delta K_{leaf_{mean}}$	Average change in leaf hydraulic conductance in response to a simulated herbivory treatment
$\Delta K_{leaf_{midrib}}$	Change in leaf hydraulic conductance 48 h after the leaf midrib has been severed
b	Xylem cell wall maximum diameter
BHPMF	Bayesian hierarchical probabilistic matrix factorization
EFM	Evaporative flux method
ER	Loop elongation ratio
ER_{large}	Loop elongation ratio in large vein sizes
ER_{medium}	Loop elongation ratio in medium vein sizes
ER_{small}	Loop elongation ratio in small vein sizes
GBM	Gradient boosting machine model
ISI	Xylem conduit implosion safety index
$K_{leaf_{max}}$	Maximum leaf hydraulic conductance
LMA	Leaf mass per area
MST	Minimum spanning tree ratio
MST_{large}	Minimum spanning tree ratio in large vein sizes
MST_{medium}	Minimum spanning tree ratio in medium vein sizes
MST_{small}	Minimum spanning tree ratio in small vein sizes
P_{50}	Leaf water potential inducing 50% loss of leaf hydraulic conductance
P_{88}	Leaf water potential inducing 88% loss of leaf hydraulic conductance
PC1	First principal component
PC2	Second principal component
PC3	Third principal component
PCA	Principal component analysis
Phe	Leaf total phenol content
r_{min}	Each value of vein width
RMSE	Root-mean-square error
SHAP	Shapley additive explanations values
SWP	Specific work to punch a leaf
SWP_{lamina}	Specific work to punch leaf lamina
SWP_{midrib}	Specific work to punch leaf midrib
SWS	Specific work to shear a leaf
SWS_{lamina}	Specific work to shear leaf lamina
SWS_{midrib}	Specific work to shear leaf midrib
tBe	Double intervessel cell wall thickness
UCBG	University of California Botanical Garden at Berkeley
UTM	Universal testing machine
VD	Vein density
VD_{large}	Vein density in large vein sizes
VD_{medium}	Vein density in medium vein sizes
VD_{small}	Vein density in small vein sizes
ε	Leaf flexural modulus of elasticity
ε_{lamina}	Leaf flexural modulus of elasticity for the leaf lamina
ε_{whole}	Leaf flexural modulus of elasticity for the whole leaf

(Niklas, 1999; Kitajima & Poorter, 2010). Quantifying the contribution of network architecture features to different leaf functions is therefore essential to understand the constraints that influenced the evolution of diverse leaf networks.

Due to the difficulty in extracting whole-leaf venation networks (but see Xu *et al.*, 2021) and in obtaining trait datasets describing all functional axes, many hypotheses relating leaf architecture and function (Fig. 2) remain to be tested. Previous studies have shown how network architecture features maximize a single (e.g. Brodribb *et al.*, 2007, 2016; Sack *et al.*, 2008; Katifori *et al.*, 2010; McKown *et al.*, 2010) or a few functional axes (Walls, 2011; Li *et al.*, 2015; Kawai & Okada, 2016, 2018, 2020; Blonder *et al.*, 2018; Hua *et al.*, 2020; Xiong & Flexas, 2022), but we still lack a more integrative picture of multidimensional trade-offs. Rather than maximizing individual functions, venation networks might be constructed to optimize overall leaf functioning. This perspective is consistent with the evolutionary hypothesis of 'multiple alternative designs' in which many phenotypes can achieve similar functioning (Wainwright, 2005; Marks & Lechowicz, 2006).

Distinguishing between these scenarios can only be assessed by simultaneously investigating multiple functional and architecture axes. In a previous study (Blonder *et al.*, 2020), we evaluated multifunctional trade-offs across vein spatial scales and found surprisingly weak relationships between venation architecture and leaf functions. However, it remained unclear if those weak trade-offs were caused by a stronger functional role of nonvenation traits or by methodological limitations. The prior study had restricted phylogenetic coverage (only 47 families, all angiosperms, all sampled from one region), incomplete networks missing major veins (networks were extracted from leaf subsections up to 2 cm^2), and insufficient trait dataset to describe all functional axes.

Here, we measured and imputed (16.8% of imputed values) leaf architecture and functional traits (Table 1) from a phylogenetically diverse set of 122 species (Supporting Information Fig. S1; Table S1). Our functional dataset included 13 traits (Table 2) and provided a more complete description of all functional axes. Our venation dataset comprised over 5 million vein segments between 10 and 500 μm of diameter, mostly (95%) extracted from whole leaves. This dataset supported an accurate representation of how key vein features (Blonder *et al.*, 2018, 2020) – vein density, vein ramification (branching vs looping), and loop geometry (circular vs elongated) (Table 3) – vary at different spatial scales within a leaf and across species. By combining those two datasets, we were able to (1) describe leaf architecture-function trade-offs, and how they vary across plant clades and vein spatial scales; (2) provide an upper bound estimate of the contribution of venation architecture to each functional axis; (3) identify which venation architecture traits at which scale (small, medium, and large vein width) predict each leaf function; and (4) determine how venation architecture traits across spatial scales interact (via independence and/or integration) to regulate leaf function. Several hypotheses have been previously advanced in the literature for the relationships within and among architecture and functional traits (Table 2). Our dataset allowed a robust assessment of those specific hypotheses (Table 2; Fig. 2) that have previously been tested with smaller datasets or not at all.

Materials and Methods

Below, we provide a brief description of how architecture and functional traits were measured. For a detailed description, see Methods S1.

New Phytologist (2024) 244: 407–425
www.newphytologist.com

Table 2 Leaf functional traits (abbreviation, unit, and definition) used as proxy for each leaf functional axes and specific hypotheses for the relationships within and among venation architecture and functional traits.

Functional axis	Proxy trait	Proxy trait definition	Venation network architecture contribution	Nonvenation architecture contribution	Hypothesis for the leaf architecture-function trade-offs
Damage resistance to drought: ability to avoid hydraulic damages (embolism, implosion) that reduce flow across the leaf	Leaf water potential inducing 50% and 88% loss of leaf hydraulic conductance – P_{50} and P_{88} (MPa)	Describes the resistance to embolism formation and propagation. Lower (more negative) P_{50} and P_{88} indicate a higher damage resistance to drought	Network's lignified structure provides resistance to hydraulic damages (implosion and embolism) during drought (Blackman *et al*., 2010; Brodribb *et al*., 2016)	Xylem pit architecture and nonxylem features (e.g. mesophyll cells permeability and fiber density) can influence resistance to embolisms and implosion (Sperry & Hacke, 2004; Scoffoni *et al*., 2023)	(H1a) Resistance to drought (Fig. 2a) should be higher in networks with lower density of larger veins, as larger veins are more prone to embolisms (i.e. formation and propagation of air bubbles inside the xylem conduits; Brodribb *et al*., 2016) under drought (Blackman *et al*., 2010). (H1b) Tree-like networks (i.e. branching networks) at small scales should be more resistant, because highly connected veins (i.e. looping networks) have more entry points for air bubbles to form and for embolisms to spread (Mrad *et al*., 2018). (H1c) Networks with more circular loops in small veins should be more resistant, because shorter conduits have less connections, thereby a lower likelihood of being in contact with an already embolized neighboring conduit from which embolisms could spread (Loepfe *et al*., 2007)
	Xylem conduit implosion safety index ISI (dimensionless)	Measures the xylem cell walls resistance to implosion during drought. The thicker the double cell wall relative to its maximum diameter (higher ISI), the greater the resistance to drought (Hacke *et al*., 2001)			
Damage resistance to herbivory: ability to avoid physical damages that reduce flow across the leaf	Specific work to punch SWP (kJ m^{-2} m^{-1})	Measures the absolute amount of work done to punch a leaf through its midrib (SWP_{midrib}) or lamina (SWP_{lamina}) per unit of leaf width (Onoda *et al*., 2011). Higher SWP indicates a higher mechanical resistance against herbivores	Network's lignified structure provides resistance to physical damages caused by herbivores (Niklas, 1999; Kitajima & Poorter, 2010)	Not only the vein architecture, but also the vein composition (e.g. fiber and sclerenchyma content) might be important to determine leaf mechanical resistance to herbivory (Roth-Nebelsick *et al*., 2001; Kitajima *et al*., 2016). Presence of foliar trichomes and antiherbivore compounds (e.g. phenols) can also increase resistance to herbivory (Agrawal & Fishbein, 2006)	(H2a) Resistance to herbivory (Fig. 2b) should be higher in networks with higher vein density (Sack & Scoffoni, 2013), particularly of larger veins (Sack *et al*., 2008). This is because veins are usually harder to break than other nonlignified leaf tissues (Kitajima & Poorter, 2010; Kawai & Okada, 2016), and larger veins are usually more sclerified and hence tougher for herbivores to damage (Choong, 1996; Roth-Nebelsick *et al*., 2001). (H2b) We also expected the presence of more circular loops at all scales to increase damage resistance, as they can provide more ways to stop the propagation of mechanical fractures, especially at leaf edges (Niklas, 1999; Fiorin *et al*., 2016). (H2c) High secondary chemistry investment (e.g. high phenol content) may offset investment in networks with high vein density and more loops
	Specific work to shear SWS (J m^{-2})	Measures the absolute amount of work done to shear the leaf midrib (SWS_{midrib}) or lamina (SWS_{lamina}) per unit of leaf width. Higher SWS indicates a higher mechanical resistance (Onoda *et al*., 2011)			

Table 2 (Continued)

Functional axis	Proxy trait	Proxy trait definition	Venation network architecture contribution	Nonvenation architecture contribution	Hypothesis for the leaf architecture-function trade-offs
Damage resilience: capacity to maintain flow through the leaf after physical or hydraulic damage has occurred	Average change in K_{leaf} after simulated herbivory in the leaf midrib and lamina $\Delta K_{leaf_{mean}}$ (%)	The percentage decrease ($\Delta K_{leaf} < 0$) or increase ($\Delta K_{leaf} > 0$) in the leaf hydraulic conductance 48 h after the leaf midrib and lamina has been physically damaged. Higher $\Delta K_{leaf_{mean}}$ indicates a higher resilience	Looping networks provide alternate transport pathways to bypass blocked or broken veins increasing leaf resilience to drought and herbivory (Sack *et al*., 2008; Katifori *et al*., 2010)	Xylem pit architecture, features related to vein leakage, and non-xylem features (e.g. mesophyll cells permeability) can also influence damage resilience (Zwieniecki *et al*., 2002; Nardini & Salleo, 2003)	(H3a) Resilience (Fig. 2c) to both drought and herbivory should be higher in networks with higher density of either small (Duarte *et al*., 2023) or large veins (Sack & Holbrook, 2006), (H3b) more looping veins at all scales (Roth-Nebelsick *et al*., 2001; Katifori *et al*., 2010), (H3c) and/or in networks with more than one primary vein emanating from the leaf base (i.e. palmate and parallel venation; Sack *et al*., 2008), as those features can provide redundant pathways that enable continued flow after damage (Sack & Scoffoni, 2013). However, very high redundancy might actually decrease resilience, by facilitating the spread of embolisms (Loepfe *et al*., 2007; Mrad *et al*., 2021) and diseases (Chatelet *et al*., 2006)
Flow efficiency: how efficiently water flows through the leaf	Maximum leaf hydraulic conductance $K_{leaf_{max}}$ (mmol m^{-2} s^{-1} MPa^{-1})	Describes how much water flows across the leaf in response to a water potential gradient between the leaf and the surrounding atmosphere (Sack & Scoffoni, 2012). Higher $K_{leaf_{max}}$ indicates a higher flow efficiency	Vein-mediated transport comprises a large fraction of total leaf conductance to water (Brodribb *et al*., 2007)	Xylem anatomical features (e.g. number and size of xylem conduits per vein) and extra-xylem tissue conductances (e.g. mesophyll and stomatal conductance) may determine a great fraction of the leaf flow efficiency (Scoffoni *et al*., 2023)	(H4a) Flow efficiency (Fig. 2d) should be higher in venation networks with a higher density of branching small veins, as small veins contribute relatively more to leaf hydraulic conductance (Sack & Holbrook, 2006; McKown *et al*., 2010; Kawai & Okada, 2016) and tree-like networks distribute resources more efficiently than networks with loops, in the absence of damage (Katifori *et al*., 2010; Fiorin *et al*., 2016)
Mechanical support: leaf capacity to remain upright in space	Leaf flexural modulus of elasticity ε (MN m^{-2})	Measures the whole leaf (ε_{whole}) or leaf lamina (ε_{lamina}) resistance to deformation from bending forces (Read *et al*., 2005; Méndez-Alonzo *et al*., 2013; Kawai & Okada, 2016). Higher ε (stiffer leaves) indicates a higher mechanical support	Network's lignified structure provides a stiff skeleton to mechanically support leaves against the pull of gravity and to remain upright in wind (Niklas, 1999)	Cuticle, epidermis, mesophyll cells (in hydrostatic leaves), and a subepidermal layer of sclerenchyma can all provide mechanical support to leaves independent of the venation network (Roth-Nebelsick *et al*., 2001; Onoda *et al*., 2015)	(H5a) Mechanical support (Fig. 2e) should be higher in networks with higher vein density, particularly of large veins (Sack & Scoffoni, 2013), as they disproportionately increase leaf stiffness (Lucas & Pereira, 1990; Choong *et al*., 1992; Choong, 1996; Onoda *et al*., 2015). (H5b) The presence of small looping veins (e.g. the small transverse veins in grass leaves), may also increase stiffness by providing reinforcing cross-linkages against bending forces (Niklas, 1999)

Table 2 (Continued)

Functional axis	Proxy trait	Proxy trait definition	Venation network architecture contribution	Nonvenation architecture contribution	Hypothesis for the leaf architecture-function trade-offs
Construction cost: total amount of resources invested in producing a leaf	Leaf mass per area LMA ($g\ m^{-2}$)	Describes the amount of resources invested on the construction of each unit of leaf area (Pérez-Harguindeguy *et al.*, 2016). Higher LMA is a proxy for a higher construction cost (Poorter *et al.*, 2009)	Lignified tissue comprising veins is costly to produce (Amthor, 2003; John *et al.*, 2017)	Specific components of leaf mass such as antiherbivore compounds (e.g. phenols) are also expensive to synthesize and may represent a large portion of the total leaf construction cost in some leaves (Chabot & Hicks, 1982). Mesophyll and epidermis anatomy and composition can also influence LMA (John *et al.*, 2017)	(H6a) Construction cost (Fig. 2f) should be higher in networks with higher vein density (Kawai & Okada, 2016), and this effect should be strongest in networks with more large veins (Niinemets *et al.*, 2007; Sack & Scoffoni, 2013; John *et al.*, 2017) due to the disproportionate scaling of cost with vein size (i.e. cost is proportional to vein radius^2)

Nonvenation features that could influence each functional axis are also presented.

Species sampling

We sampled 122 species (Table S1) from the living collections of the University of California Botanical Garden at Berkeley (37.87°N, 122.23°W; CA, USA). Our samples included woody and herbaceous species, with origins from all continents except Antarctica, but growing under similar conditions as in a 'common garden' experiment (Perez *et al.*, 2019). For each species, branches (> 1 m long, woody species) or whole plants (herbaceous species) were sampled from 1 to 5 mature individuals, re-cut under water, re-hydrated overnight, and then used for the measurement of functional (Table 2) and architecture traits (Table 3). As most measurements were destructive, different leaves were used for each trait. This sampling approach where the number of replicates within species is reduced to achieve a broader phylogenetic coverage allowed us to investigate trait variation at higher taxonomic levels (clades and families), but had less power at lower levels (genus and species).

Leaf functional traits

Flow efficiency was quantified as the maximum leaf hydraulic conductance ($K_{leaf_{max}}$, mmol $m^{-2}\ s^{-1}\ MPa^{-1}$). $K_{leaf_{max}}$ was measured on 4–10 leaves per species using the evaporative flux method (EFM, Sack & Scoffoni, 2012) with a pressure-drop flow meter (Melcher *et al.*, 2012). EFM more closely approximates the transpiration flow of an *in vivo* leaf (Sack & Scoffoni, 2012), as it involves evaporating water out of the lamina while determining the flow rate into the petiole with a flow meter (model PX26-001GV; Omega Engineering, Norwalk, CT, USA) and the water potential drop across the leaf with a pressure chamber (model 1505D; PMS, Albany, OR, USA).

Damage resistance to drought was measured as the leaf water potentials inducing 50% (P_{50}, MPa) and 88% (P_{88}, MPa) loss of $K_{leaf_{max}}$ using the EFM (Sack & Scoffoni, 2012; Scoffoni *et al.*, 2012). To describe xylem resistance to implosion, we also measured xylem conduits' implosion safety index (ISI, dimensionless) from 6 to 8 leaf cross-sectional anatomical images per species, including images of the petiole, major and minor veins (Matos *et al.*, 2024). For each image, xylem cell wall maximum diameter (b) and double intervessel cell wall thickness (t) were manually measured on all or, at most, 10 adjacent xylem conduits using the software ImageJ (https://imagej.nih.gov/). ISI was calculated as t/b (Hacke *et al.*, 2001; Blackman *et al.*, 2010).

Damage resistance to herbivory was quantified as the specific work to punch (SWP, kJ $m^{-2}\ m^{-1}$) and to shear (SWS, J m^{-2}) a leaf (3–4 leaves per species) using a universal testing machine (UTM, Test stand ES30 and force gauge series M5; Mark-10, Copiague, NY, USA). Punching tests involved forcing a rod of known cross-sectional area through the leaf midrib or lamina, whereas shearing tests involved using a single blade to make a transverse cut across the leaf midrib and lamina (Read *et al.*, 2005; Onoda *et al.*, 2011). We also quantified the total phenol content (Phe, g g^{-1}) in dried leaves using the Folin–Ciocalteu assay (Ainsworth & Gillespie, 2007). Phe can be used as a partial proxy of chemical defense against herbivores (Matsuki, 1996).

Table 3 Leaf venation architecture traits (abbreviation, unit and definition).

Leaf venation architecture traits	Definition	High trait value for small veins	Low trait value for small veins
Vein density (VD, mm mm^{-2})	Length of all vein segments per unit of leaf area. Higher VD indicates more veins per unit leaf area	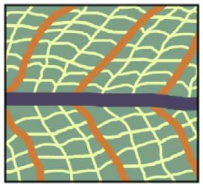	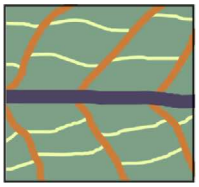
Minimum spanning tree ratio (MST, dimensionless)	Degree of branching vs looping in the network. Calculated by computing the length of the minimum spanning tree connecting all vein junctions divided by the length of all veins. Higher MST indicates a more branching (tree-like) network with fewer loops	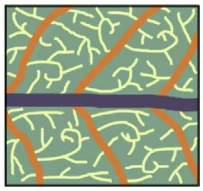	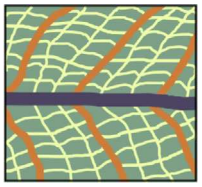
Loop elongation ratio (ER, dimensionless)	How elongated the loops are. Calculated by fitting an ellipse to each loop, and dividing the major axis length by the minor axis length, then taking the median ratio across all loops and subtracting 1 (for statistical convenience). Higher ER indicates more elongated (less circular) loops	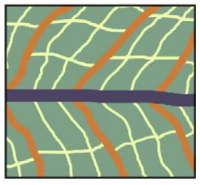	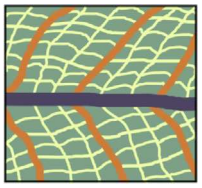

The example illustrations show networks with high or low values of each venation architecture traits for the small veins only (yellow lines), while features of medium (orange) and large (purple) veins remain constant. In reality, variation in architecture traits can occur across all scales (small, medium, and large veins).

Damage resilience was quantified as the average change in leaf hydraulic conductance ($\Delta K_{leaf_{mean}}$, %) after the lamina or the midrib(s) were cut at one-third distance from the leaf base (Delaney & Higley, 2006; Sack *et al.*, 2008). Severing treatments subjected leaves to both physical/herbivory (because of the cut) and hydraulic/drought (because air could enter through the cut conduits) damages (Sack *et al.*, 2008; Peschiutta *et al.*, 2016). Forty-eight hours after treatment, we excised the damaged leaves and measured K_{leaf} using the EFM. ΔK_{leaf} was calculated separately for the midrib and lamina, that is $\Delta K_{leaf} = [(\Delta K_{leaf_{midrib}}$ or $\Delta K_{leaf_{lamina}} \times 100)/K_{leaf_{max}}] - 100$, and then averaged for each sample to obtain $\Delta K_{leaf_{mean}}$. $\Delta K_{leaf_{mean}} < 0$ indicates lower resilience (i.e. K_{leaf} declines after damage), while $\Delta K_{leaf_{mean}} \geq 0$ indicates higher resilience.

Mechanical support was described by the leaf flexural modulus of elasticity (ε, MN m^{-2}; Read *et al.*, 2005), measured on 3–4 leaves per species using the UTM. For each leaf, 3-point bending tests were conducted twice, to obtain ε for the whole leaf (ε_{whole}), and leaf lamina (ε_{lamina}). Leaves were placed in the UTM with their longitudinal axis parallel to the bending fixture.

Construction cost was described as the leaf mass per area (LMA, g m^{-2}), measured in 3–5 mature leaves per species. Leaves were first scanned to obtain leaf area, and then oven-dried at 50°C for 48 h to determine their dry mass (B2-Series; VWR, Radnor, PA, USA). LMA was then calculated as leaf dry mass/leaf area (Pérez-Harguindeguy *et al.*, 2016).

ISI, LMA, SWP_{lamina} and $K_{leaf_{max}}$ were measured in all 122 species. For various reasons (Methods S1), missing data occurred for the other functional traits, with variable percentages of missing values ranging from 1% (Phe) to 74% (P_{50} and P_{88}). Therefore, caution must be used when interpreting the results for those last two traits.

Leaf venation architecture traits

To obtain the architecture traits, leaves were pressed flat, dried, and chemically cleared and stained to highlight veins (Blonder *et al.*, 2018; Pérez-Harguindeguy *et al.*, 2016). Next, cleared leaf samples were imaged using a 100-mm macro-objective lens (Tokina, Huntington Beach, CA, USA) and digital camera (EOS 6D; Canon, Southend-on-Sea, UK) or a *trans*illuminated scanner (Epson Perfection V850 Pro, Los Alamitos, CA, US), producing high-resolution images (47–144 pixels mm^{-1}) of the whole leaf. This process resolved veins ≥10 μm in diameter. Therefore, all larger veins were accurately imaged in all species, but in species with minor venation smaller than this threshold, the architecture traits at smaller spatial scales missed some veins.

Leaf images were processed using the LeafVeinCNN software, v.1.3 and newer (Xu *et al.*, 2021; software and manual available from doi: 10.5281/zenodo.4007731). LeafVeinCNN relies on an ensemble of three convolutional neural networks to automatically

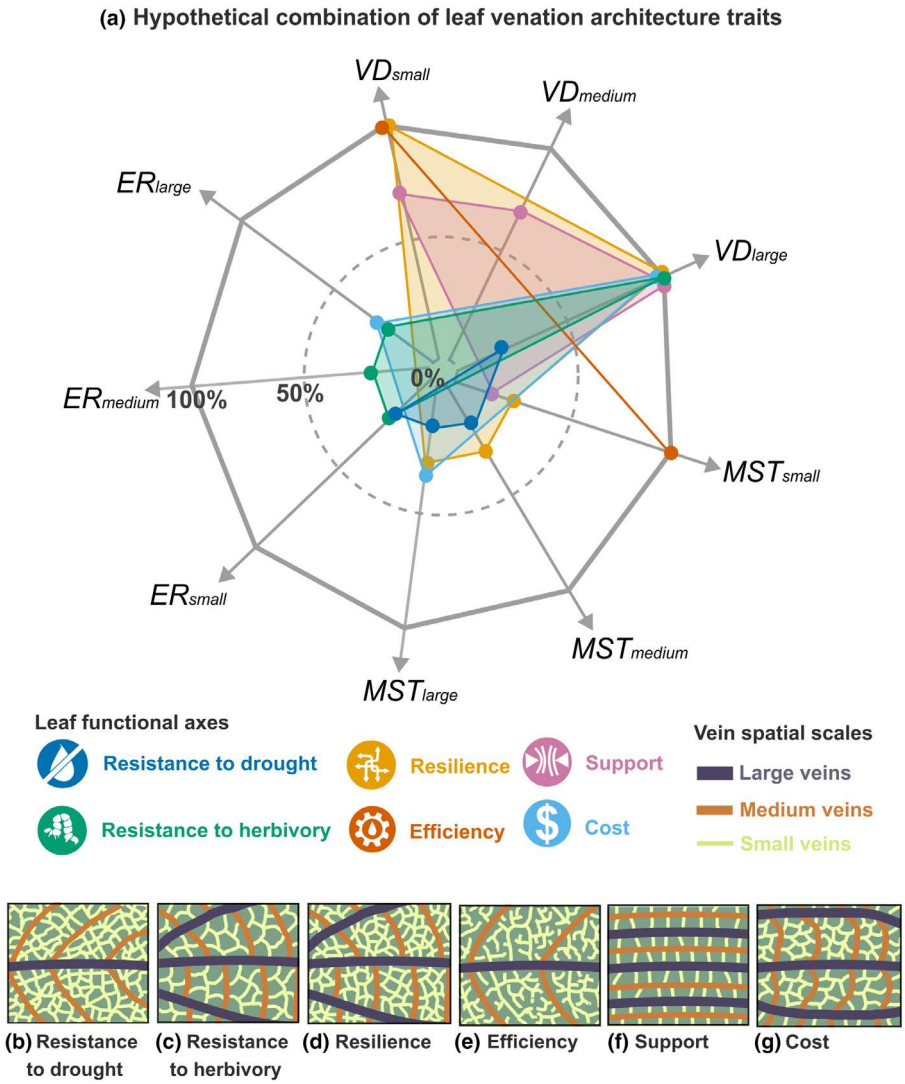

Fig. 2 Hypothesized combinations of leaf venation architecture traits (ER, loop elongation ratio; MST, minimum spanning tree ratio; VD, vein density) at three vein spatial scales (small, medium, and large) that would have evolved if each leaf functional axis was independently optimized: (a) Radar chart of hypothesized trait combinations. (b) Damage resistance to drought should be higher in networks with lower density of large veins (low VD_{large}), branching large and medium veins (low MST_{large} and MST_{medium}), and more circular loops in small veins (low ER_{small}); (c) Damage resistance to herbivory should be higher in networks with higher large vein density (high VD_{large}) and more circular loops at all scales (low ER); (d) Damage resilience to drought and herbivory should be higher in networks with higher density of large and small veins (high VD_{small} and VD_{large}), palmate venation (more than one midrib), and more loops (low MST) at all scales; (e) Flow efficiency should be higher in networks with higher density (high VD_{small}) of branching (high MST_{small}) small veins; (f) Mechanical support should be higher in networks with higher large vein density (high VD_{large}) and more loops in small veins (low MST_{small}); and (g) Construction cost should be higher in networks with higher density (high VD_{large} and VD_{medium}) of large and medium veins.

segment veins and produce a spatial graph representation of the networks. The program also uses hierarchical loop decomposition algorithms (Katifori & Magnasco, 2012) to extract multiscale venation statistics, which describe how venation architecture traits vary across spatial scales (Blonder *et al.*, 2020), that is across each value of vein width (r_{min}). We focused our analysis on three statistics–vein density (VD), minimum spanning tree ratio (MST), and loop elongation ratio (ER) (Table 3) – previously identified as key traits to describe venation architecture (Blonder *et al.*, 2018, 2020).

Extensive quality control steps, including additional hand-tracing in some samples, followed standard protocols, ensuring the accuracy of the segmented networks and the multiscale statistics. Architecture traits could not be obtained for two species (*Aucuba japonica* Thunb. and *Nymphaea* sp.) because chemical treatments failed to properly digest nonvenation tissues. In seven monocot species, leaves were too long (> 30 cm) to be fully processed, so a leaf segment representing *c.* 20–50% of the total leaf area was analyzed.

Statistical analysis

To evaluate whether species in different clades and/or veins at different sizes occupy different portions of the architecture-function space (Goal 1), we carried out a principal component analysis (PCA) with all traits. Before the PCA, we imputed missing values (Methods S1) using a Bayesian hierarchical probabilistic matrix factorization (BHPMF; Schrodt *et al.*, 2015). BHPMF imputes values based on the taxonomic hierarchy and correlation structure within the trait matrix. Briefly, we $\log_{10}$- and *z*-transformed all trait values, performed 50 imputations (Table S2), filtered out implausible values, and then calculated the mean and SD of the imputed values. To validate the imputation, we regressed original vs imputed values and evaluated the R^2 (Methods S1). Next, venation traits (VD, ER, and MST) were binned into 50 r_{min} bins, spanning 0.01 mm ($r_{min} < 0.01$ mm, veins too small to be distinguishable) to 0.5 mm ($r_{min} > 0.5$ mm, too few veins sampled, see Fig. S2). Finally, trait values were centered and scaled (*z*-transformed) to improve comparability and reduce bias

toward traits with higher variance. VD and ER were also square-root-transformed to improve normality. The broken-stick method was used to determine the principal components to be retained. The retained principal components were visualized using 95% confidence ellipses at each clade and at each r_{min}.

To quantify the contribution of architecture traits to each function (Goal 2), we fitted gradient boosting machine (GBM) models. GBM is a machine-learning ensemble method that effectively captures complex nonlinear interactions between predictor variables (Natekin & Knoll, 2013). We fitted our models using one functional trait at a time as the response variable, and clade plus architecture traits as predictor variables. To make an interpretable assessment of the contribution of architecture traits at different spatial scales, we binned VD, MST, and ER at three scales to represent small, medium, and large veins. Because the range of vein sizes vary across leaves, we used two complementary approaches (scaled and unscaled r_{min}) to classify veins into size categories (Methods S1), allowing us to investigate how both relative (scaled r_{min}) and absolute veins sizes (unscaled r_{min}) influence architecture-function trade-offs. To fit each GBM, we split data 80%/20% between training and test sets. Then, we used the *h2o.automl* function as implemented in the *h2o* R-package to perform a hyperparameter search over the GBM parameters. To prevent model overfitting, hyperparameter tuning was done with a maximum running time of 30 s and a threefold cross-validation. Model performance was assessed using root-mean-square error (RMSE), and the best model (lowest RMSE) for each functional trait was selected using the function *h2o.get_best_model*. From each best model, we obtained the total variance explained as an estimate of the contribution of venation architecture traits to each functional axis (Goal 2). Due to the lower sample size ($n = 32$), GBM models for P_{50} and P_{88} were fitted using both the complete-case and the BHPMF-imputed datasets. To account for the uncertainty around the imputed values, we ran 50 GBM models for P_{50} and P_{88}, using imputed values obtained in each of the 50 imputations. We report the GBM results averaged across those iterations.

To identify which architecture traits at which scale predict leaf functions (Goal 3), we obtained the influence value of each predictor variable in each best GBM model. Variable influence was obtained using both permutation importance and SHapley Additive exPlanation (SHAP) values (Štrumbelj & Kononenko, 2014). Variable importance, ranging from 0 (lowest importance) to 1 (highest importance), was determined using the *h2o.varimp* function, which measures the increase in the model RMSE after variable values are permuted. To compare the importance of predictor variables between the best model and the other GBM models fitted with the same data, we used the function *h2o.varimp_heatmap*, which produces a heatmap of variable importance across multiple GBM models. SHAP values were determined using *h2o.predict_contributions* function, and they measure the impact of every predictor variable on the model prediction for each instance of the data. Thus, predictor variables with larger absolute SHAP values have a larger contribution to explain the response variable.

To determine how architecture traits across scales interact to predict leaf functions (Goal 4), we measure the strength of pairwise interactions using the H-statistic (Friedman & Popescu, 2008), as implemented in *Interaction$new* from the *iml* R-package. *H*-statistics measure how much of the variation of the predicted outcome depends on a given pairwise interaction and vary from 0 (no interaction) to 1 (100% of variance is due to interactions).

To test for differences in functional traits across plant clades, and to test our hypothesis H3c (Table 2) that resilience varies across venation types (parallel, palmate, and pinnate), we used phylogenetic ANOVA tests followed by *post hoc* pairwise tests with Benjamini & Hochberg (1995) *P*-value adjustments. Phylogenetic ANOVA tests were implemented following Garland Jr. *et al.* (1993) using the function *phyloANOVA* from the PHYTOOLS R-package. All analyses were carried out using R v.4.3.1 (R Core Team, 2023). R code to reproduce all analyses is available at: https://github.com/ilamatos/venation_tradeoffs/.

Results

Leaf functional and architecture traits vary across species and scales

We found substantial variation in functional traits across species (Tables S1–S3). For example, LMA varied *c.* 15-fold across species (from 18.91 to 276.20 g m^{-2}), while $K_{leaf_{max}}$ varied *c.* 232-fold (from 0.15 to 34.83 mmol m^{-2} s^{-1} MPa^{-1}). SWP_{midrib} was on average (226.08 kJ m^{-2} m^{-1}) *c.* 2× higher than SWP_{lamina} (128.83 kJ m^{-2} m^{-1}). By contrast, SWS_{lamina} (6309 J m^{-2}) and ε_{lamina} (78.77 MN m^{-2}) were on average *c.* 3× higher than SWS_{midrib} (2316 J m^{-2}) and ε_{whole} (28.66 MN m^{-2}). When leaf midrib(s) and lamina were damaged, $K_{leaf_{max}}$ decreased on average by *c.* 55%. However, some species ($n = 11$) experienced an increase in $\Delta K_{leaf_{mean}}$ (from 0.07% up to *c.* 295%). When we applied phylogenetic ANOVA tests to compare functional traits across clades, we found significant differences only in SWS_{lamina}, which was lower in basal eudicot species (Fig. S3).

Architecture traits demonstrated high variation among species and clades (Figs S4–S6), and complex patterns across vein sizes. As r_{min} increased, VD decreased (Fig. S4) and MST increased (Fig. S5), whereas ER peaked at intermediate r_{min} values (Fig. S6), reflecting a tendency of more veins and loops at smaller spatial scales, and more elongated loops at medium-sized veins.

Leaf architecture-function trade-offs are in general weak

Principal component analysis identified three significant axes (Fig. S5), which cumulatively explained 44% of the total variation (Figs 3, S8), suggesting weak generalized architecture-function trade-offs across vein scales and plant phylogeny. Despite the fundamental differences in drought- and herbivory-induced damages (the former can spread across the network while the latter may not), resistance to both factors covaried along the first principal component (PC1, Fig. 3). Leaves on the left PC1 side have high resistance against both herbivory (higher SWP) and drought (more negative P_{88}), while leaves on the right PC1 side have low resistance (Tables S4, S5). Architecture

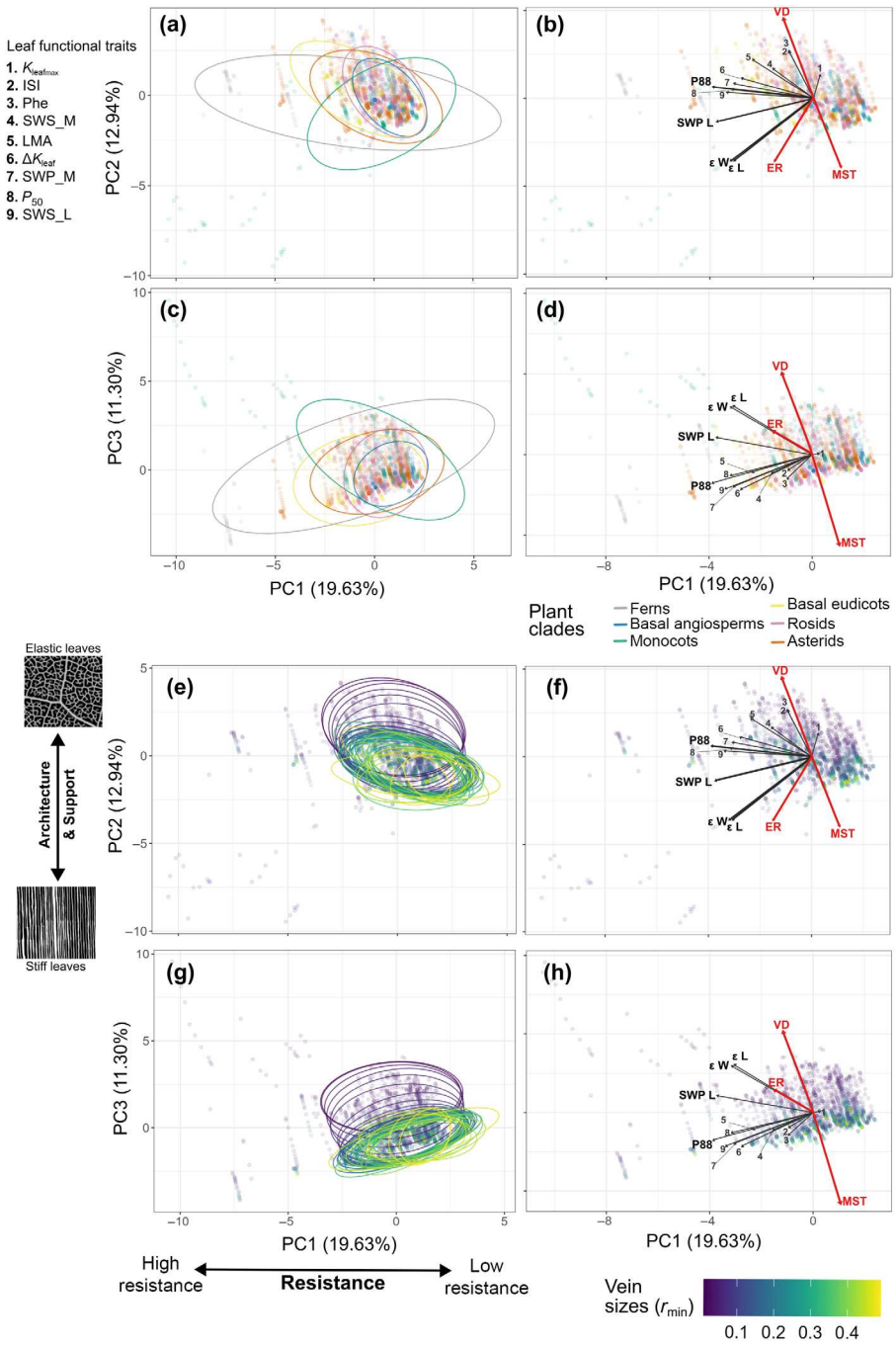

Fig. 3 First (PC1), second (PC2), and third (PC3) principal components of leaf venation architecture (VD, MST, ER, colored in red) and functional traits ($K_{leaf_{max}}$, P_{50}, P_{88}, ISI, SWP_{midrib}, SWP_{lamina}, SWS_{midrib}, SWS_{lamina}, $\Delta K_{leaf_{mean}}$, ε_{whole}, ε_{lamina}, LMA, Phe, colored in black) across 50 bins of vein width sizes (r_{min}). In panels (a, c, e, g), the 95% confidence ellipses enclose the data at each plant phylogenetic clade (ferns, basal angiosperms, monocots, basal eudicots, rosids, and asterids), or at each vein spatial scale (r_{min}). Panels (b, d, f, h) show the principal component analysis loadings. Note that leaf architecture traits (shown in red) vary across vein sizes (r_{min}), while functional traits (shown in black) do not. The main loadings for PC1, PC2, and PC3 are shown in bold. Other trait loadings are numbered from 1 to 9. Parenthetical values indicate the percentage variance explained by the three first principal component axes. Trait abbreviations: ER, elongation ratio; ISI, Implosion safety index; $K_{leaf_{max}}$, maximum leaf hydraulic conductance; LMA, leaf mass per area; MST, minimum spanning tree ratio; P_{50}, leaf water potential inducing 50% loss of $K_{leaf_{max}}$; P_{88}, leaf water potential inducing 88% loss of $K_{leaf_{max}}$; Phe, Phenol content; SWP_L, specific work to punch the leaf lamina; SWP_M, specific work to punch the midrib; SWS_L, specific work to shear the lamina; SWS_M, specific work to shear the midrib; VD, vein density; ΔK_{leaf}, mean change in $K_{leaf_{max}}$ after damaging the leaf lamina and midrib; ε_L, leaf flexural modulus of elasticity for the leaf lamina; ε_W, leaf flexural modulus of elasticity for the whole leaf.

traits had a low contribution to PC1 (Table S4). PC2 reflected a network architecture-support axis (Fig. 3). Leaves at the upper PC2 axis are more elastic (lower ε) and have a high density (higher VD) of small veins (lower r_{min}) forming circular loops (lower ER and MST), while leaves at the bottom PC2 axis show an opposite combination of traits. PC3 further reflected the trade-off between VD and MST (Fig. S8). Fern species spread along PC1, reflecting their broad range of drought and herbivory resistances, whereas monocots spread along PC2 reflecting the existence of different venation architectures (e.g. parallel and palmate) within this clade (Fig. 3). Vein sizes (r_{min}) differentiated along PC2 (Fig. 3) and PC3 (Fig. S8), reflecting the tendency of small veins (lower r_{min}) to have higher density and more circular loops.

Venation architecture traits contribute to leaf support, cost, and resistance

Architecture traits plus clade explained half or more of the total variance (Fig. 4) for traits describing mechanical support, cost, and resistance but had a lower explanatory power for determining leaf resilience and efficiency. Except for Phe and SWS_{midrib}, the

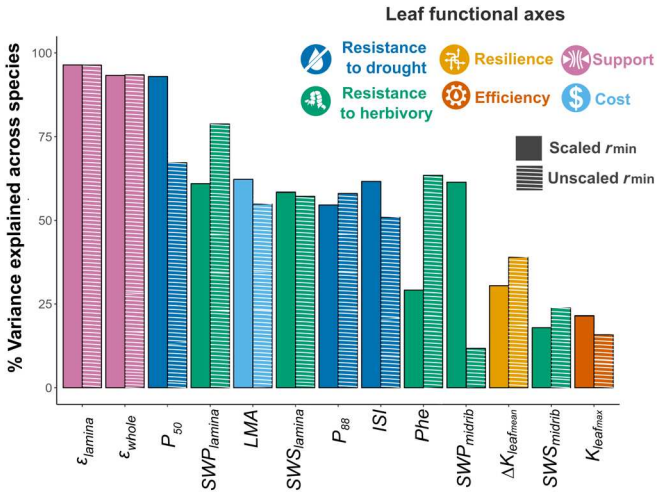

Fig. 4 Results of gradient boosting machine (GBM) assessing variation in architecture (predictor variables) and functional (response variables) trade-offs across vein spatial scales (small, medium, and large veins) and plant phylogeny (clade). The total percentage of variance explained by the best GBM model indicates how much the variance in venation architecture traits across species contribute to explain the variance in 13 leaf functional traits (P_{50}, P_{88}, ISI, SWP_{midrib}, SWP_{lamina}, SWS_{midrib}, SWP_{lamina}, $\Delta K_{leaf_{mean}}$, $K_{leaf_{max}}$, ε_{whole}, ε_{lamina}, LMA, Phe) describing six functional axes (resistance to drought, resistance to herbivore, resilience, flow efficiency, mechanical support, and construction cost). All models were run with complete-case dataset and either with scaled (scaled r_{min}) or unscaled (unscaled r_{min}) vein sizes. Trait abbreviations: ISI, Implosion safety index; $K_{leaf_{max}}$, maximum leaf hydraulic conductance; LMA, leaf mass per area; P_{50}, leaf water potential inducing 50% loss of $K_{leaf_{max}}$; P_{88}, leaf water potential inducing 88% loss of $K_{leaf_{max}}$; Phe, Phenol content; SWP_{lamina}, specific work to punch the leaf lamina; SWP_{midrib}, specific work to punch the midrib; SWS_{lamina}, specific work to shear the lamina; SWS_{midrib}, specific work to shear the midrib; $\Delta K_{leaf_{mean}}$, mean change in $K_{leaf_{max}}$ after damaging the leaf lamina and midrib; ε_{lamina}, leaf flexural modulus of elasticity for the leaf lamina; ε_{whole}, leaf flexural modulus of elasticity for the whole leaf.

variance explained was similar in models using absolute (unscaled r_{min}) and relative (scaled r_{min}) vein sizes. For P_{50} and P_{88}, variance explained was higher in models ran with complete-case (Fig. 4), than with imputed trait values (R^2: $P_{50_{scaled}} = 0.30$; $P_{50_{unscaled}} = 0.32$; $P_{88_{scaled}} = 0.23$; $P_{50_{unscaled}} = 0.62$). Tables S6 and S7 show hyperparameters values for the best selected models and performance metrics for all GBM models, respectively.

Venation architecture contribution to leaf function vary across spatial scales

Architecture traits at different spatial scales contributed to different leaf functions (Fig. S9). Overall, clade was not ranked as an important variable to explain variation in most of the functional traits, suggesting that architecture-function trade-offs vary more within rather than between clades. The order of predictor variables' importance changed between GBM models based on the absolute or relative vein sizes (Fig. S9), and between different GBM models fitted using the same data (Figs S10, S11). But, in most cases, the direction of the predictor variables' effect on the response variable was similar across different models.

The impact of each predictor variable on each functional trait is displayed in the SHAP summary plots (Figs 5, S12, S13). In the SHAP plot, each point represents an instance of data (i.e. one species). The point color indicates the normalized value of the corresponding predictor variable, with pink indicating high values and blue indicating low values. The *y*-axis shows the top five (from top to bottom) predictor variables most important to explain the response variable. The *x*-axis represents the SHAP contribution values. SHAP signal indicates whether the predictor variable increases (SHAP > 0) or decreases (SHAP < 0) the response variable, while SHAP magnitude measures how strong this positive or negative impact is. Thus, a SHAP value around zero indicates that the predictor variable has an irrelevant effect on the response variable, while a larger absolute SHAP value indicates a greater effect. For example, in Fig. 5(c), loop elongation in small veins (ER_{small}) followed by MST_{medium} and MST_{large} were the three most important variables to explain interspecific variation in leaf resistance to herbivory described as SWP_{lamina}. Species with more elongated loops in small veins (i.e. higher ER_{small} indicated by the pink-colored points on the right side of the ER_{small} row) tend to exhibit higher resistance to herbivory (higher SWP_{lamina} indicated by the more positive SHAP values). Additionally, species with more loops on medium size veins (i.e. lower MST_{medium} indicated by the blue-colored points) are associated with higher SWP_{lamina} values (more positive SHAP values). By contrast, species with more loops in large size veins (i.e. lower MST_{large}) are associated with lower SWP_{lamina} (more negative SHAP values). Those results only partially support our hypothesis (H2), as we found no strong evidence that higher density of large veins contributes to higher resistance to herbivory (Figs S12, S13). Phe was associated with networks of higher vein density and more circular loops at all scales (Figs S12, S13). Contrary to H2c, we found no evidence that high investment in secondary chemistry offsets investment in physical defense provided by the lignified network.

Contrary to our expectations (H1a and H1c), resistance to drought was higher in networks with higher density of larger veins and with intermediary values of ER (Figs 5a, S12, S13). As expected (H1b), more tree-like small veins resulted in higher resistance to drought, but this effect was weak. Because of the greater uncertainty associated with the imputed P_{50} and P_{88} values (Table S2), when we averaged the results across the 50 GBM imputed-based models, we basically found no clear effect of venation architecture traits on drought resistance (Fig. S14).

Resilience was higher in networks with higher density of large veins and either high or low density of small veins, thus partially supporting H3a (Figs 5d, S12, S13). $\Delta K_{leaf_{mean}}$ was also higher in networks with intermediate values of ER_{medium} and ER_{large}, more loops in large veins, and more branching minor veins, thus partially supporting H3b. Contrary to H3c, we found no significant differences in $\Delta K_{leaf_{mean}}$ ($F = 0.2322$, P-value $= 0.906$), $\Delta K_{leaf_{midrib}}$ ($F = 0.3716$, P-value $= 0.841$), or $\Delta K_{leaf_{lamina}}$ ($F = 0.0802$, P-value $= 0.968$), between palmate, pinnate, and parallel leaves.

As hypothesized (H4a), flow efficiency was higher in networks with higher density of small veins (Figs 5b, S12, S13). However, higher $K_{leaf_{max}}$ was found in networks with intermediate, rather

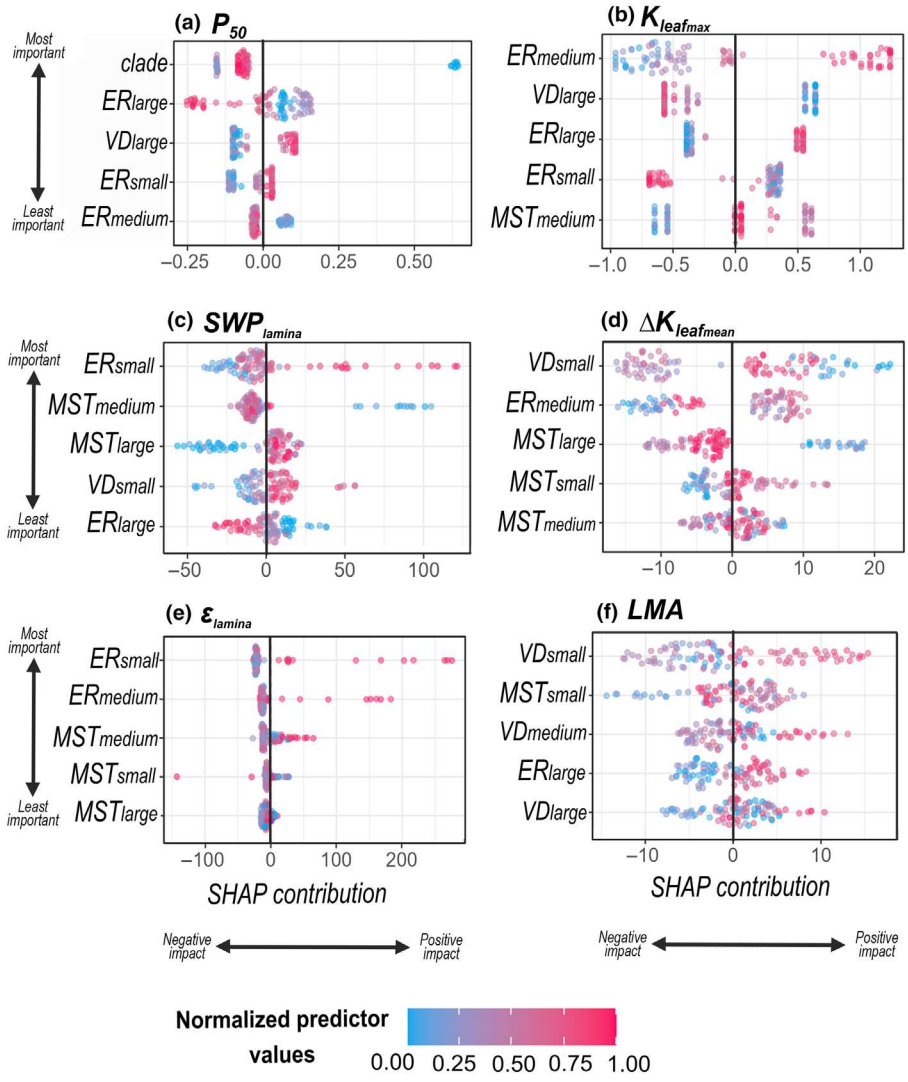

Fig. 5 SHapley Additive exPlanations (SHAP) summary plots for six leaf functional axes. SHAP values measure the impact of predictor variables (i.e. plant clades and vein density (VD), loop elongation ratio (ER), and minimum spanning tree ratio (MST) at three spatial scales – large, medium, and small) on the response variables (leaf functional traits) considering the interactions between predictors. (a) Resistance to drought – P_{50} (leaf water potential inducing 50% decline in leaf hydraulic conductance), (b) Efficiency – $K_{leaf_{max}}$ (maximum leaf hydraulic conductance), (c) Resistance to herbivory – SWP_{lamina} (specific work to shear leaf lamina), (d) Resilience – $\Delta K_{leaf_{mean}}$ (percentage decline in leaf hydraulic conductance after damage), (e) Mechanical support – ε_{lamina} (leaf flexural modulus of elasticity for the leaf lamina), (f) Construction cost – leaf mass per area. Note that this figure only presents SHAP values for the top five most important predictor variables, and for just one functional trait per functional axis. Complete SHAP summary plots for all 13 functional traits measured in this study are shown in Fig. S11. All results present here were run with complete-case dataset and unscaled r_{min} (i.e. absolute vein sizes), for the scaled r_{min} (i.e. relative vein sizes) results, see Fig. S12. For traits abbreviations, see Table 1.

than low MST_{small} and more elongated loops in medium and large veins.

Mechanical support was higher in networks with more looping small veins and higher large vein density, although in some species high VD_{large} was associated with lower ε_{whole}, thus only partially supporting H5a. The presence of elongated loops in medium veins was also important to explain ε in our dataset (Figs 5e, S12, S13). Note that those relationships were highly influenced by a few monocot species with parallel venation and high elasticity. As expected (H6a), construction cost was higher in leaf networks with higher vein density, but this effect was not particularly strong for large veins (Figs 5f, S12, S13). Fig. 6 summarizes the results for the architecture-function trade-offs across the six leaf functional axes.

Venation architecture traits across spatial scales interact weakly to regulate leaf function

Overall, pairwise interactions between predictor variables were weak (Fig. S15), with H-statistic < 0.3 (Table S8), suggesting low integration across architecture traits at different vein orders. Fig. S15 shows the strongest interactions in our dataset for the GBM models with scaled and unscaled r_{min}, respectively.

Discussion

Overall, we found that: (1) generalized leaf architecture-function trade-offs across vein spatial scales and plant phylogeny are weak; (2) architecture traits play a stronger role on leaf mechanical support and damage resistance, than on flow efficiency and damage resilience; (3) architecture traits at different spatial scales contribute to different leaf functions, which potentially reduces the necessity of trade-offs among functional axes driven by venation architecture; and (4) pairwise interactions between architecture traits both at a single scale (e.g. $VD_{large} \times ER_{large}$) and across spatial scales (e.g. $VD_{small} \times VD_{large}$) are weak, reflecting no widespread trade-offs among different aspects of network architecture.

Those results suggest that given the existence of different constraints (e.g. biophysical, physiological, and phylogenetic) leaf venation networks reflect a compromise among multiple competing functions (Ronellenfitsch *et al.*, 2015; Patino-Ramirez & Arson, 2020). This means that no single optimal venation

network exists, but instead, there might be multiple trait combinations or alternative designs of network architectures (Wainwright, 2005; Marks & Lechowicz, 2006) that can be deployed to achieve equivalent overall functioning. The independence of venation architecture traits within and across vein spatial scales, reflected by the weak pairwise interactions in our dataset, could allow more freedom for adjusting traits and functioning to the environment (Li *et al.*, 2015; Méndez-Alonzo *et al.*, 2019). This perspective contrasts with prior conclusions about leaf venation in which it was proposed that single functions were optimized (Sack & Tyree, 2005; Zwieniecki *et al.*, 2006; Noblin *et al.*, 2008; Deans *et al.*, 2020) and reinforces recent ideas about the high dimensionality of adaptation in plants (Baraloto *et al.*, 2010; He *et al.*, 2020). This means that species may achieve similar levels of function in the same environment despite dissimilar venation architectures. Because leaf functions are determined not only by network architecture but also by multiple biochemical, anatomical, morphological, and physiological venation and nonvenation traits operating at different spatial scales (Table 2), there could be numerous trait combinations yielding similar functioning. Each leaf represents the realization of one viable combination among those multiple possibilities. Thus, it is not surprising that we failed to identify strong and widespread architecture-function trade-offs across the plant phylogeny. Nevertheless, we did find clear linkages between venation architecture and leaf functions, particularly for mechanical support, damage resistance, and cost. We discuss how variation in key venation architecture traits across spatial scales influence each leaf functional axis independently, even though leaf networks are likely selected for achieving sufficient performance in each functional axis, rather than an optimum performance in any single function.

Influence of venation architecture on each leaf function

Damage resistance to drought: Although larger veins seem to be more prone to embolisms (Brodribb *et al.*, 2016; Scoffoni *et al.*, 2017b), we found that networks with a higher density of larger veins may be more resistant to drought. This result was supported by previous empirical studies (Scoffoni *et al.*, 2011; Nardini *et al.*, 2014; Xiong & Flexas, 2022) and could be explained by the concept of relative leverage between veins (Sack & Scoffoni, 2013). When VD_{large} is higher, large veins have less leverage relative to the small vein system, and embolisms in major veins should cause a smaller decrease in K_{leaf}. Conversely, when VD_{small} is higher, large veins gain leverage, and embolisms in large veins should cause great loss of conductance. Therefore, since embolisms typically begin in the largest veins and progresses into smaller ones (Brodribb *et al.*, 2016; Scoffoni *et al.*, 2017b), a higher VD_{large} is likely more effective for reducing overall leaf hydraulic vulnerability to drought than a higher VD_{small} (Sack & Scoffoni, 2013). Thus, despite the overall trend of independence among architecture traits, in some circumstances, a coordination in network architecture across spatial scales could be important to maximizing some leaf functions (Kawai & Okada, 2018).

Damage resistance to herbivory was overall higher in networks with small veins forming circular loops (lower ER_{small} and MST_{small}), corroborating the hypothesis that reticulation in small veins can increase deterrence against chewing/cutting damage by providing more ways to stop the propagation of mechanical fractures (Niklas, 1999; Fiorin *et al.*, 2016). However, contrary to previous studies, we found no evidence that a higher density of large veins increases damage resistance to herbivory (Sack *et al.*, 2008; Kitajima & Poorter, 2010; Kawai & Okada, 2016) nor that a high investment in chemical defense can offset investment in mechanical resistance by the lignified network (Blonder *et al.*, 2020; Duarte *et al.*, 2023). Importantly, we did not directly measure herbivory attack nor did we quantify other secondary metabolites important for chemical defenses against herbivory, so those hypotheses cannot be completely ruled out.

Mechanical support was largely explained by venation architecture features, and higher in networks with higher density of larger veins and more looping small veins. Those results corroborate previous studies showing that larger and more sclerified veins can increase leaf stiffness (Onoda *et al.*, 2015; Kawai & Okada, 2016) as they act as beams that support the leaf weight (Niklas, 1999), while more reticulated small veins can increase stiffness by providing reinforcing cross-linkages that resist mechanical loading (Niklas, 1999; Roth-Nebelsick *et al.*, 2001). Importantly, in our dataset, the architecture-function trade-offs along the mechanical support axis were largely influenced by monocot species with parallel venation and stiff leaves. In those species, the parallel arrangement of the large veins, reinforced with small transverse veins, leads to a very efficient stabilization of the leaf against bending forces (Roth-Nebelsick *et al.*, 2001). We also found a novel result that more elongated medium veins increase leaf stiffness, perhaps because they form cross-links between primary and secondary veins, helping to stabilize the whole leaf in the same way that triangular trusses stabilize bridges.

Construction cost was associated with high densities of both small and large veins, indicating that even though minor veins usually occupy a small volume inside the leaf (Sack & Scoffoni, 2013), they may still impact the final leaf cost, probably due to their more than fourfold higher tissue density compared with mesophyll and epidermis tissues (Poorter *et al.*, 2009). Those results contradict previous studies showing that leaf construction cost and the densities of both major and minor veins form independent axes (Kawai & Okada, 2020). Our work, based on a larger and more phylogenetically diverse dataset, suggests that venation architecture features are important in explaining variation in leaf cost across species, and do not form independent axes in the architecture-function space.

Damage resilience: Overall, venation architecture traits had a low contribution to this functional axis. Resilience was slightly higher in networks with a high density of looping large veins. This architecture design may increase resilience by providing more redundant pathways for continued long-distance flow after damages (Sack *et al.*, 2008; Katifori *et al.*, 2010). More loops in small veins, however, decreased resilience, probably because too much reticulation in small veins can lead to a faster spread of embolisms (Loepfe *et al.*, 2007; Mrad *et al.*, 2021). By contrast,

less reticulation may increase resilience by restricting damages to a single conduit or group of conduits (Sack & Scoffoni, 2013) and maybe also by facilitating embolism repair (Schenk *et al.*, 2008). Therefore, optimal architecture for resilience may occur when networks combine high redundancy (more loops) in major veins with high sectoriality (less loops) in minor veins. In contrast to Sack *et al.* (2008), we found no difference in resilience between palmate, pinnate, and parallel leaves. This is probably

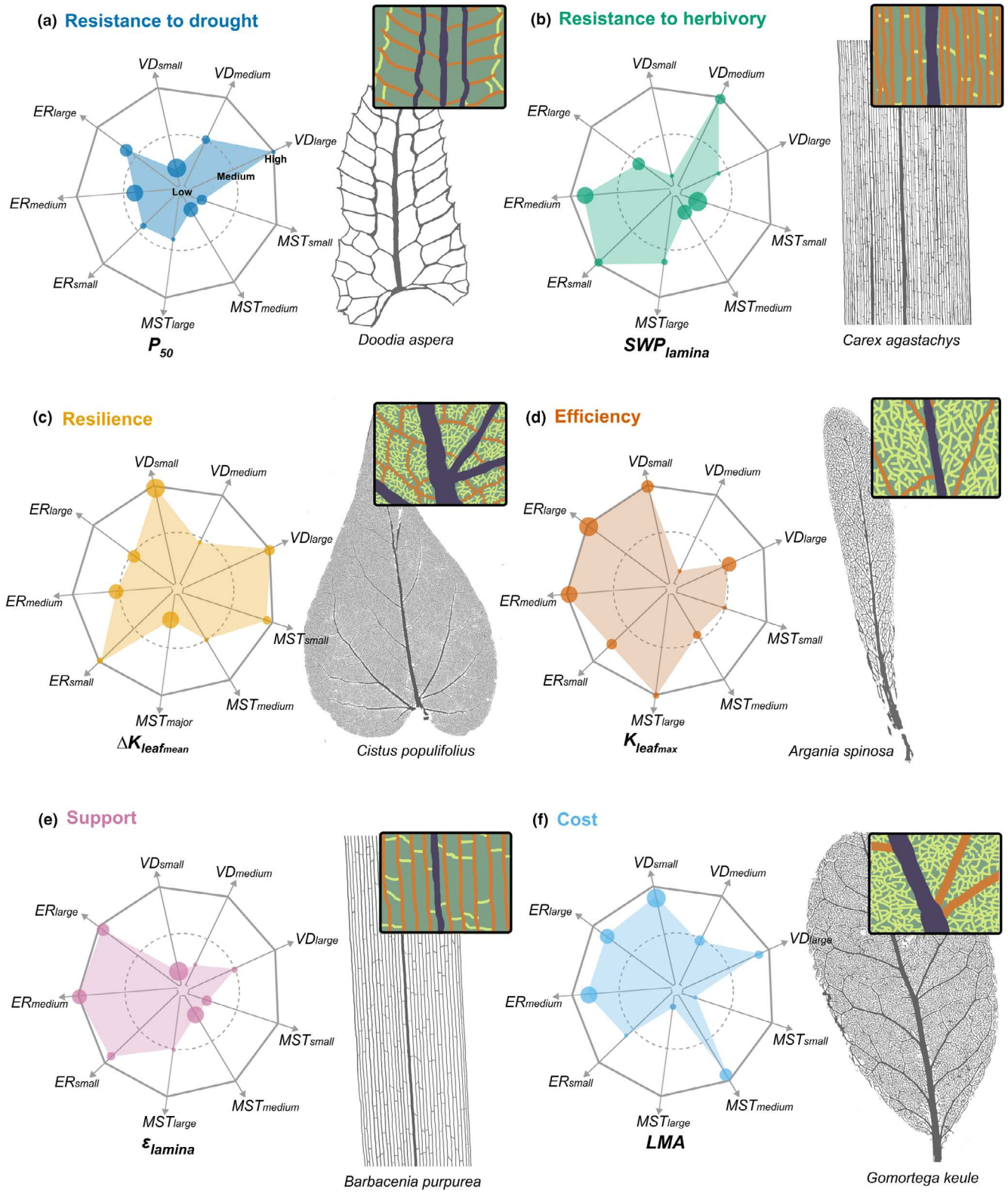

Fig. 6 Radar charts, based on observed data, for the combination of leaf venation architecture traits (ER, elongation ratio; MST, minimum spanning tree ration; VD, vein density) at three vein spatial scales (small, medium, large) that maximizes each leaf functional axis independently: (a) Resistance to drought – P_{50} P_{50} (leaf water potential inducing 50% decline in leaf hydraulic conductance), (b) Resistance to herbivory – SWP_{lamina} (specific work to shear leaf lamina), (c) Resilience – $\Delta K_{leaf_{mean}}$ (percentage decline in leaf hydraulic conductance after damage), (d) Efficiency – $K_{leaf_{max}}$ (maximum leaf hydraulic conductance), (e) Mechanical support – ε_{lamina} (leaf flexural modulus of elasticity for the leaf lamina), (f) Construction cost – leaf mass per area. In the radar charts, point sizes indicate the predictor variable importance, with bigger points reflecting higher importance; whereas the point position along the predictor variable axis (low, medium, and high) indicates the SHapley Additive exPlanation value contribution. For each functional axis, we also show a hand-selected example of a real leaf venation network that approximates this 'optimum' combination of leaf venation architecture traits. Zoom insets for each image show small, medium, and large veins as light green, orange, and purple lines, respectively. For traits abbreviations, see Table 1.

because Sack *et al.* (2008) only damaged the midvein of palmately veined species, while we severed all midribs, canceling out any extra redundancy provided by having multiple primary veins. In both studies, treatments were an explicitly mechanical simulation of herbivory and did not include chemical signaling pathways (Waterman *et al.*, 2019) that may impact K_{leaf} changes in response to herbivory.

Flow efficiency was only weakly influenced by venation architecture, suggesting that leaf hydraulics might be highly controlled by venation anatomical traits or outside-venation traits (Caringella *et al.*, 2015; Xiong & Flexas, 2022; Scoffoni *et al.*, 2023). Theoretically, venation networks with high MST_{small} (i.e. tree-like minor veins) should achieve the highest water supply rate for a given investment of veins in the absence of damages (Corson, 2010; Katifori *et al.*, 2010). In our study, however, higher $K_{leaf_{max}}$ was found in networks with intermediate MST_{small}, perhaps because real leaves are constantly subjected to damage, and so they need to optimize not only the flow efficiency, but also resilience/resistance to damages. Importantly, flow efficiency may be more related to the architecture traits of very minor veins (i.e. veins with width < 0.01 mm), which were missing in our dataset. This could be another reason for the weak relationships between flow efficiency and venation architecture in our study.

Limitations and future directions

In this study, we were unable to assess veins with width < 10 μm. Thus, our estimation of small vein features' contribution to leaf functions may be biased. Future work should merge venation architecture statistics estimated from high-resolution images of whole leaves with those obtained from microscopic images of leaf subsections to better assess traits at different vein spatial scales. Another limitation is that our P_{50} and P_{88} values obtained using the EFM method cannot differentiate K_{leaf} declines caused by xylem embolisms from those caused by changes in the permeability of outside-xylem tissues (Sack & Scoffoni, 2012). Furthermore, due to methodological issues related to sample size (i.e. P_{50} and P_{88} were only measured on 32 out of 122 species), our results linking venation architecture and resistance to embolisms are provisional and need to be further explored. To better quantify the contribution of venation features to damage resistance during drought, future research should combine different methods that quantify how both inside- (Brodribb *et al.*, 2016; Scoffoni *et al.*, 2017a) and outside-xylem changes (Scoffoni *et al.*, 2023) influence the whole-leaf resistance under increasing water stress.

Conclusions

Variation in leaf venation architecture features across spatial scales was important to determine different leaf functions, especially mechanical support, damage resistance, and cost. However, due to the high dimensionality of the functional space, generalized leaf architecture-function trade-offs across the plant phylogeny were weak. Multiple combinations of venation and nonvenation traits were found to achieve equivalent functional performance. The absence of generalized rules linking leaf architecture-function observed here challenges prior studies that have proposed simple and generalizable models of leaf functioning. To further understand the rules linking leaf network architecture and function, future studies should focus on (1) quantifying the contribution of both inside- and outside-xylem traits on the different leaf functional axes, particularly damage resilience and flow efficiency; (2) investigating whether alternative metrics of network architecture not assessed here (e.g. vein orientation and connectivity, Mrad *et al.*, 2021) may have stronger functional linkages; (3) constructing mechanistic models (e.g. Buckley *et al.*, 2017) to determine the venation network architectures that are optimal under selection for different combinations of functions and costs; and (4) identifying the macroevolutionary causes of variation in network architecture across clades.

Acknowledgements

We are grateful to all staff of the University of California Botanical Garden at Berkeley for the logistical support, especially to the horticulturists Ethan Fenner, Eric Hupperts, James Fong, Noah Gapsis, Gideon Dollarhide, Sophia Warsh, Jason Bonham, Corina Rieder, and the Director of Research & Collections Vanessa Handley who helped us with sample collection. We thank Denise Schines for sharing histological and microscopy methods. We also thank Prof. Cynthia Looy and Prof. Todd Dawson for lending their equipment to obtain the leaf anatomical dataset. We thank Haley Grimmer and Nguyen Huynh for their help measuring leaf architecture and functional traits. Undergraduate students that worked in this project were supported either by UC Berkeley programs: Undergraduate Research Apprentice Program (URAP) and Sponsored Projects for Undergraduate Research (SPUR), or by the United States National Science Foundation (NSF) programs: Research Experience for Undergraduates (REU), Research Experience for Teachers (RET), and Research Experience for Post-Baccalaureate Students (REPS). This study

was supported by the US National Science Foundation (grant NSF-DEB-2025282), the University of California at Berkeley, and the Natural Environment Research Council (NERC/NE/M019160/1).

Competing interests

None declared.

Authors contributions

BWB and MF acquired funding. ISM and BWB designed the study. HF provided logistical support to access the University of California Botanical Garden living collections and research glasshouse. ISM, MB, SC, AF, LG, JR and JT collected leaf samples and obtained the functional dataset. IN, AC, AE, SM, SC and NY prepared cleared leaf images for network extraction. ISM, BCJ, DK, JR, MA and SM obtained the leaf anatomical dataset. MF developed the program for leaf venation extraction, which was improved by SS and SM. ISM, BV, JM, MS and CT extracted leaf venation networks and obtained the leaf venation architectural dataset. ISM analyzed the data and drafted the manuscript. All authors contributed to and revised the manuscript.

ORCID

Monica Antonio https://orcid.org/0009-0009-0662-0511
Benjamin Wong Blonder https://orcid.org/0000-0002-5061-2385
Mickey Boakye https://orcid.org/0000-0002-6557-9928
Ashley Chu https://orcid.org/0009-0008-1096-853X
Mark Fricker https://orcid.org/0000-0002-8942-6897
Diana Kalantar https://orcid.org/0009-0009-2233-163X
Joseph Mann https://orcid.org/0009-0008-3082-9123
Ilaine Silveira Matos https://orcid.org/0000-0001-5557-5133
Izzi Niewiadomski https://orcid.org/0009-0003-9288-6063
Meg Scudder https://orcid.org/0009-0006-4791-758X
Connor Tomaka https://orcid.org/0000-0002-5939-1638
Nicole Yokota https://orcid.org/0009-0009-7295-2266

Data availability

The leaf trait dataset, including both leaf venation network architecture and functional traits, as well as high-resolution cleared leaf images, and venation segmentations are permanently archived on Dryad repository at doi: 10.5061/dryad.1g1jwsv36. Algorithms to analyze images and to calculate multiscale statistics are available in Xu *et al.* (2021). R-code to reproduce all analysis are available at https://github.com/ilamatos/venation_tradeoffs/.

References

Agrawal AA, Fishbein M. 2006. Plant defense syndromes. *Ecology* **87**: S132–S149.

Ainsworth EA, Gillespie KM. 2007. Estimation of total phenolic content and other oxidation substrates in plant tissues using Folin–Ciocalteu reagent. *Nature Protocols* **2**: 875–877.

Amthor JS. 2003. Efficiency of lignin biosynthesis: a quantitative analysis. *Annals of Botany* **91**: 673–695.

Baraloto C, Timothy Paine CE, Poorter L, Beauchene J, Bonal D, Domenach A-M, Hérault B, Patiño S, Roggy J-C, Chave J. 2010. Decoupled leaf and stem economics in rain forest trees: decoupled leaf and stem economics spectra. *Ecology Letters* **13**: 1338–1347.

Benjamini Y, Hochberg Y. 1995. Controlling the false discovery rate: a practical and powerful approach to multiple testing. *Journal of the Royal Statistical Society, Series B: Statistical Methodology* **57**: 289–300.

Blackman CJ, Brodribb TJ, Jordan GJ. 2010. Leaf hydraulic vulnerability is related to conduit dimensions and drought resistance across a diverse range of woody angiosperms. *New Phytologist* **188**: 1113–1123.

Blonder B, Both S, Jodra M, Xu H, Fricker M, Matos IS, Majalap N, Burslem DFRP, Teh YA, Malhi Y. 2020. Linking functional traits to multiscale statistics of leaf venation networks. *New Phytologist* **228**: 1796–1810.

Blonder B, Salinas N, Bentley LP, Shenkin A, Chambi Porroa PO, Valdez Tejeira Y, Boza Espinoza TE, Goldsmith GR, Enrico L, Martin R *et al.* 2018. Structural and defensive roles of angiosperm leaf venation network reticulation across an Andes–Amazon elevation gradient. *Journal of Ecology* **106**: 1683–1699.

Boyce CK, Brodribb TJ, Feild TS, Zwieniecki MA. 2009. Angiosperm leaf vein evolution was physiologically and environmentally transformative. *Proceedings of the Royal Society B: Biological Sciences* **276**: 1771–1776.

Brodribb TJ, Bienaimé D, Marmottant P. 2016. Revealing catastrophic failure of leaf networks under stress. *Proceedings of the National Academy of Sciences, USA* **113**: 4865–4869.

Brodribb TJ, Feild TS, Jordan GJ. 2007. Leaf maximum photosynthetic rate and venation are linked by hydraulics. *Plant Physiology* **144**: 1890–1898.

Brodribb TJ, Feild TS, Sack L. 2010. Viewing leaf structure and evolution from a hydraulic perspective. *Functional Plant Biology* **37**: 488–498.

Buckley TN, John GP, Scoffoni C, Sack L. 2017. The sites of evaporation within leaves. *Plant Physiology* **173**: 1763–1782.

Caringella MA, Bongers FJ, Sack L. 2015. Leaf hydraulic conductance varies with vein anatomy across *Arabidopsis thaliana* wild-type and leaf vein mutants. *Plant, Cell & Environment* **38**: 2735–2746.

Chabot BF, Hicks DJ. 1982. The ecology of leaf life spans. *Annual Review of Ecology and Systematics* **13**: 229–259.

Chatelet DS, Matthews MA, Rost TL. 2006. Xylem structure and connectivity in grapevine (*Vitis vinifera*) shoots provides a passive mechanism for the spread of bacteria in grape plants. *Annals of Botany* **98**: 483–494.

Choong MF. 1996. What makes a leaf tough and how this affects the pattern of Castanopsis fissa leaf consumption by caterpillars. *Functional Ecology* **10**: 668.

Choong MF, Lucas PW, Ong JSY, Pereira B, Tan HTW, Turner IM. 1992. Leaf fracture toughness and sclerophylly: their correlations and ecological implications. *New Phytologist* **121**: 597–610.

Corson F. 2010. Fluctuations and redundancy in optimal transport networks. *Physical Review Letters* **104**: 48703.

Deans RM, Brodribb TJ, Busch FA, Farquhar GD. 2020. Optimization can provide the fundamental link between leaf photosynthesis, gas exchange and water relations. *Nature Plants* **6**: 1116–1125.

Delaney KJ, Higley LG. 2006. An insect countermeasure impacts plant physiology: midrib vein cutting, defoliation and leaf photosynthesis. *Plant, Cell & Environment* **29**: 1245–1258.

Duarte MA, Woo S, Hultine K, Blonder B, Aparecido LMT. 2023. Vein network redundancy and mechanical resistance mitigate gas exchange losses under simulated herbivory in desert plants. *AoB Plants* **15**: plad002.

Fiorin L, Brodribb TJ, Anfodillo T. 2016. Transport efficiency through uniformity: organization of veins and stomata in angiosperm leaves. *New Phytologist* **209**: 216–227.

Friedman JH, Popescu BE. 2008. Predictive learning via rule ensembles. *Annals of Applied Statistics* **2**: 148.

Fujita H, Mochizuki A. 2006. The origin of the diversity of leaf venation patterns. *Developmental Dynamics* **235**: 2710–2721.

Garland T Jr, Dickerman AW, Janis CM, Jones JA. 1993. Phylogenetic analysis of covariance by computer simulation. *Systematic Biology* **42**: 265–292.

Hacke UG, Sperry JS, Pockman WT, Davis SD, McCulloh KA. 2001. Trends in wood density and structure are linked to prevention of xylem implosion by negative pressure. *Oecologia* **126**: 457–461.

He N, Li Y, Liu C, Xu L, Li M, Zhang J, He J, Tang Z, Han X, Ye Q *et al.* 2020. Plant trait networks: improved resolution of the dimensionality of adaptation. *Trends in Ecology & Evolution* **35**: 908–918.

Hua L, He P, Goldstein G, Liu H, Yin D, Zhu S, Ye Q. 2020. Linking vein properties to leaf biomechanics across 58 woody species from a subtropical forest. *Plant Biology* **22**: 212–220.

John GP, Scoffoni C, Buckley TN, Villar R, Poorter H, Sack L. 2017. The anatomical and compositional basis of leaf mass per area. *Ecology Letters* **20**: 412–425.

Katifori E, Magnasco MO. 2012. Quantifying loopy network architectures. *PLoS ONE* **7**: e37994.

Katifori E, Szöllősi GJ, Magnasco MO. 2010. Damage and fluctuations induce loops in optimal transport networks. *Physical Review Letters* **104**: 48704.

Kawai K, Okada N. 2016. How are leaf mechanical properties and water-use traits coordinated by vein traits? A case study in Fagaceae. *Functional Ecology* **30**: 527–536.

Kawai K, Okada N. 2018. Roles of major and minor vein in leaf water deficit tolerance and structural properties in 11 temperate deciduous woody species. *Trees* **32**: 1573–1582.

Kawai K, Okada N. 2020. Leaf vascular architecture in temperate dicotyledons: correlations and link to functional traits. *Planta* **251**: 17.

Kitajima K, Poorter L. 2010. Tissue-level leaf toughness, but not lamina thickness, predicts sapling leaf lifespan and shade tolerance of tropical tree species. *New Phytologist* **186**: 708–721.

Kitajima K, Wright SJ, Westbrook JW. 2016. Leaf cellulose density as the key determinant of inter- and intra-specific variation in leaf fracture toughness in a species-rich tropical forest. *Interface Focus* **6**: 20150100.

Li L, McCormack ML, Ma C, Kong D, Zhang Q, Chen X, Zeng H, Niinemets Ü, Guo D. 2015. Leaf economics and hydraulic traits are decoupled in five species-rich tropical-subtropical forests. *Ecology Letters* **18**: 899–906.

Loepfe L, Martinez-Vilalta J, Piñol J, Mencuccini M. 2007. The relevance of xylem network structure for plant hydraulic efficiency and safety. *Journal of Theoretical Biology* **247**: 788–803.

Lucas PW, Pereira B. 1990. Estimation of the fracture toughness of leaves. *Functional Ecology* **4**: 819.

Marks CO, Lechowicz MJ. 2006. Alternative designs and the evolution of functional diversity. *The American Naturalist* **167**: 55–66.

Matos IS, McDonough S, Johnson BC, Kalantar D, Rohde J, Sahu R, Wang J, Fontao A, To J, Carlos S *et al.* 2024. Negative allometry of leaf xylem conduit diameter and double-wall thickness: implications for implosion safety. *New Phytologist* **242**: 2464–2478.

Matsuki M. 1996. Regulation of plant phenolic synthesis: from biochemistry to ecology and evolution. *Australian Journal of Botany* **44**: 613.

McKown AD, Cochard H, Sack L. 2010. Decoding leaf hydraulics with a spatially explicit model: principles of venation architecture and implications for its evolution. *The American Naturalist* **175**: 447–460.

Melcher PJ, Michele Holbrook N, Burns MJ, Zwieniecki MA, Cobb AR, Brodribb TJ, Choat B, Sack L. 2012. Measurements of stem xylem hydraulic conductivity in the laboratory and field: measurements of stem xylem hydraulic conductivity. *Methods in Ecology and Evolution* **3**: 685–694.

Méndez-Alonzo R, Ewers FW, Jacobsen AL, Pratt RB, Scoffoni C, Bartlett MK, Sack L. 2019. Covariation between leaf hydraulics and biomechanics is driven by leaf density in Mediterranean shrubs. *Trees* **33**: 507–519.

Méndez-Alonzo R, Ewers FW, Sack L. 2013. Ecological variation in leaf biomechanics and its scaling with tissue structure across three mediterranean-climate plant communities. *Functional Ecology* **27**: 544–554.

Mrad A, Domec J, Huang C, Lens F, Katul G. 2018. A network model links wood anatomy to xylem tissue hydraulic behaviour and vulnerability to cavitation. *Plant, Cell & Environment* **41**: 2718–2730.

Mrad A, Johnson DM, Love DM, Domec J. 2021. The roles of conduit redundancy and connectivity in xylem hydraulic functions. *New Phytologist* **231**: 996–1007.

Nardini A, Õunapuu-Pikas E, Savi T. 2014. When smaller is better: leaf hydraulic conductance and drought vulnerability correlate to leaf size and venation density across four Coffea arabica genotypes. *Functional Plant Biology* **41**: 972–982.

Nardini A, Salleo S. 2003. Effects of the experimental blockage of the major veins on hydraulics and gas exchange of *Prunus laurocerasus* L. leaves. *Journal of Experimental Botany* **54**: 1213–1219.

Natekin A, Knoll A. 2013. Gradient boosting machines, a tutorial. *Frontiers in Neurorobotics* **7**: 21.

Niinemets U, Portsmouth A, Tobias A. 2007. Leaf shape and venation pattern alter the support investments within leaf lamina in temperate species: a neglected source of leaf physiological differentiation? *Functional Ecology* **21**: 28–40.

Niklas KJ. 1999. A mechanical perspective on foliage leaf form and function. *New Phytologist* **143**: 19–31.

Noblin X, Mahadevan L, Coomaraswamy IA, Weitz DA, Holbrook NM, Zwieniecki MA. 2008. Optimal vein density in artificial and real leaves. *Proceedings of the National Academy of Sciences, USA* **105**: 9140–9144.

Onoda Y, Schieving F, Anten NPR. 2015. A novel method of measuring leaf epidermis and mesophyll stiffness shows the ubiquitous nature of the sandwich structure of leaf laminas in broad-leaved angiosperm species. *Journal of Experimental Botany* **66**: 2487–2499.

Onoda Y, Westoby M, Adler PB, Choong AMF, Clissold FJ, Cornelissen JHC, Díaz S, Dominy NJ, Elgart A, Enrico L *et al.* 2011. Global patterns of leaf mechanical properties: global patterns of leaf mechanical properties. *Ecology Letters* **14**: 301–312.

Patino-Ramirez F, Arson C. 2020. Transportation networks inspired by leaf venation algorithms. *Bioinspiration & Biomimetics* **15**: 36012.

Perez TM, Valverde-Barrantes O, Bravo C, Taylor TC, Fadrique B, Hogan JA, Pardo CJ, Stroud JT, Baraloto C, Feeley KJ. 2019. Botanic gardens are an untapped resource for studying the functional ecology of tropical plants. *Philosophical Transactions of the Royal Society, B: Biological Sciences* **374**: 20170390.

Pérez-Harguindeguy N, Díaz S, Garnier E, Lavorel S, Poorter H, Jaureguiberry P, Bret-Harte MS, Cornwell WK, Craine JM, Gurvich DE *et al.* 2016. Corrigendum to: New handbook for standardised measurement of plant functional traits worldwide. *Australian Journal of Botany* **64**: 715.

Peschiutta ML, Bucci SJ, Scholz FG, Goldstein G. 2016. Compensatory responses in plant-herbivore interactions: impacts of insects on leaf water relations. *Acta Oecologica* **73**: 71–79.

Poorter H, Niinemets Ü, Poorter L, Wright IJ, Villar R. 2009. Causes and consequences of variation in leaf mass per area (LMA): a meta-analysis. *New Phytologist* **182**: 565–588.

Price CA, Enquist BJ, Savage VM. 2007. A general model for allometric covariation in botanical form and function. *Proceedings of the National Academy of Sciences, USA* **104**: 13204–13209.

R Core Team. 2023. *R: a language and environment for statistical computing.* Vienna, Austria: R Foundation for Statistical Computing. [WWW document] URL https://www.R-project.org/ [accessed 10 February 2024].

Read J, Sanson GD, Lamont BB. 2005. Leaf mechanical properties in sclerophyll woodland and shrubland on contrasting soils. *Plant and Soil* **276**: 95–113.

Ronellenfitsch H, Katifori E. 2019. Phenotypes of vascular flow networks. *Physical Review Letters* **123**: 248101.

Ronellenfitsch H, Lasser J, Daly DC, Katifori E. 2015. Topological phenotypes constitute a new dimension in the phenotypic space of leaf venation networks. *PLoS Computational Biology* **11**: e1004680.

Roth-Nebelsick A, Uhl D, Mosbrugger V, Kerp H. 2001. Evolution and function of leaf venation architecture: a review. *Annals of Botany* **87**: 553–566.

Sack L, Dietrich EM, Streeter CM, Sánchez-Gómez D, Holbrook NM. 2008. Leaf palmate venation and vascular redundancy confer tolerance of hydraulic disruption. *Proceedings of the National Academy of Sciences, USA* **105**: 1567–1572.

Sack L, Holbrook NM. 2006. Leaf hydraulics. *Annual Review of Plant Biology* **57**: 361–381.

Sack L, Scoffoni C. 2012. Measurement of leaf hydraulic conductance and stomatal conductance and their responses to irradiance and dehydration using the Evaporative Flux Method (EFM). *Journal of Visualized Experiments* **20**: 4179.

Sack L, Scoffoni C. 2013. Leaf venation: structure, function, development, evolution, ecology and applications in the past, present and future. *New Phytologist* **198**: 983–1000.

Sack L, Tyree MT. 2005. Leaf hydraulics and its implications in plant structure and function. In: *Vascular transport in plants*. Cambridge, MA, USA: Elsevier, 93–114.

Savage VM, Bentley LP, Enquist BJ, Sperry JS, Smith DD, Reich PB, Von Allmen EI. 2010. Hydraulic trade-offs and space filling enable better predictions of vascular structure and function in plants. *Proceedings of the National Academy of Sciences, USA* **107**: 22722–22727.

Schenk HJ, Espino S, Goedhart CM, Nordenstahl M, Cabrera HIM, Jones CS. 2008. Hydraulic integration and shrub growth form linked across continental aridity gradients. *Proceedings of the National Academy of Sciences, USA* **105**: 11248–11253.

Schrodt F, Kattge J, Shan H, Fazayeli F, Joswig J, Banerjee A, Reichstein M, Bönisch G, Díaz S, Dickie J *et al.* 2015. BHPMF–a hierarchical Bayesian approach to gap-filling and trait prediction for macroecology and functional biogeography: gap-filling in trait databases. *Global Ecology and Biogeography* **24**: 1510–1521.

Scoffoni C, Albuquerque C, Brodersen CR, Townes SV, John GP, Bartlett MK, Buckley TN, McElrone AJ, Sack L. 2017a. Outside-xylem vulnerability, not xylem embolism, controls leaf hydraulic decline during dehydration. *Plant Physiology* **173**: 1197–1210.

Scoffoni C, Albuquerque C, Brodersen CR, Townes SV, John GP, Cochard H, Buckley TN, McElrone AJ, Sack L. 2017b. Leaf vein xylem conduit diameter influences susceptibility to embolism and hydraulic decline. *New Phytologist* **213**: 1076–1092.

Scoffoni C, Albuquerque C, Buckley TN, Sack L. 2023. The dynamic multi-functionality of leaf water transport outside the xylem. *New Phytologist* **239**: 2099–2107.

Scoffoni C, McKown AD, Rawls M, Sack L. 2012. Dynamics of leaf hydraulic conductance with water status: quantification and analysis of species differences under steady state. *Journal of Experimental Botany* **63**: 643–658.

Scoffoni C, Rawls M, McKown A, Cochard H, Sack L. 2011. Decline of Leaf Hydraulic conductance with dehydration: relationship to leaf size and venation architecture. *Plant Physiology* **156**: 832–843.

Sperry JS, Hacke UG. 2004. Analysis of circular bordered pit function I. Angiosperm vessels with homogenous pit membranes. *American Journal of Botany* **91**: 369–385.

Štrumbelj E, Kononenko I. 2014. Explaining prediction models and individual predictions with feature contributions. *Knowledge and Information Systems* **41**: 647–665.

Ueno O, Kawano Y, Wakayama M, Takeda T. 2006. Leaf vascular systems in C_3 and C_4 grasses: a two-dimensional analysis. *Annals of Botany* **97**: 611–621.

Wainwright PC. 2005. Many-to-one mapping of form to function: a general principle in organismal design? *Integrative and Comparative Biology* **45**: 256–262.

Walls RL. 2011. Angiosperm leaf vein patterns are linked to leaf functions in a global-scale data set. *American Journal of Botany* **98**: 244–253.

Waterman JM, Cazzonelli CI, Hartley SE, Johnson SN. 2019. Simulated herbivory: the key to disentangling plant defense responses. *Trends in Ecology & Evolution* **34**: 447–458.

Xiong D, Flexas J. 2022. Safety–efficiency tradeoffs? Correlations of photosynthesis, leaf hydraulics, and dehydration tolerance across species. *Oecologia* **200**: 51–64.

Xu H, Blonder B, Jodra M, Malhi Y, Fricker M. 2021. Automated and accurate segmentation of leaf venation networks via deep learning. *New Phytologist* **229**: 631–648.

Zwieniecki MA, Melcher PJ, Boyce CK, Sack L, Holbrook NM. 2002. Hydraulic architecture of leaf venation in *Laurus nobilis* L.: hydraulic architecture of leaf venation. *Plant, Cell & Environment* **25**: 1445–1450.

Zwieniecki MA, Stone HA, Leigh A, Boyce CK, Holbrook NM. 2006. Hydraulic design of pine needles: one-dimensional optimization for single-vein leaves. *Plant, Cell & Environment* **29**: 803–809.

Supporting Information

Additional Supporting Information may be found online in the Supporting Information section at the end of the article.

Fig. S1 Phylogenetic tree for 122 species.

Fig. S2 Number of samples (species) with a vein present at each vein spatial scale (r_{min}).

Fig. S3 Variation in leaf functional traits of 122 plant species across clades.

Fig. S4 Vein density variation across vein spatial scales.

Fig. S5 Minimum spanning tree ratio variation across vein spatial scales.

Fig. S6 Loop elongation ratio variation across vein spatial scales.

Fig. S7 Eigenvalues (gray bars) for each principal component with null model values generated by the broken-stick model (red line).

Fig. S8 Results of principal component analysis of leaf venation architecture and functional traits across 50 classes of vein diameter sizes.

Fig. S9 Heat maps showing the scaled importance of each predictor variable.

Fig. S10 Heat maps showing variation across models in the importance of predictor variables using scaled vein sizes.

Fig. S11 Heat maps showing variation across models in the importance of predictor variables using unscaled vein sizes.

Fig. S12 SHapley Additive exPlanation summary plots using unscaled vein sizes.

Fig. S13 SHapley Additive exPlanation summary plots using scaled vein sizes.

Fig. S14 Variable importance and SHapley Additive exPlanation values using imputed P_{50} and P_{88} trait values.

Fig. S15 Strength of interactions between predictor variables.

Methods S1 Supplementary methods.

Table S1 List of 122 plant species evaluated in this study.

Table S2 Imputed values for 14 leaf functional traits.

Table S3 Summary statistics of leaf venation architecture and functional traits.

Table S4 Principal component loadings for the leaf venation architecture and functional traits across 16 principal components.

Table S5 Principal component (PC) scores for the three first PCs for each of the 120 plant species across 50 vein width sizes (r_{min}) bins.

Table S6 Best gradient boosted models selected for each leaf functional trait.

Table S7 Performance metrics for all gradient boosted models.

Table S8 Strength (*H*-statistic) of pairwise interactions.

Please note: Wiley is not responsible for the content or functionality of any Supporting Information supplied by the authors. Any queries (other than missing material) should be directed to the *New Phytologist* Central Office.